Exploration and Detection of Subsurface Water Using Broadband Electromagnetic Sensors

T. DAVID MCGLONE

Smoke Creek Instruments, Inc., P.O. Box 169, Golden, CO 80402

ABSTRACT ●

Because of water's conductivity properties, electromagnetic geophysical surveys are often used in the detection and monitoring of subsurface water. The common coil receiver is a simple and inexpensive instrument that measures the derivative of the magnetic field strength. It has a frequency bandwidth dependent on its physical geometry and a frequency-dependent amplitude response. Generally, these instruments have a limited useful frequency response, requiring different sets of coils if information over more than a few discrete frequencies within a narrow bandwidth is desired.

The use of wide bandwidth receivers in electromagnetic geophysical surveys can provide information that limited bandwidth instruments can not. A magnetic field receiver with a small physical size allows array measurements of electromagnetic fields in a manner similar to arrays used for seismic measurements. This makes feasible 2-D and 3-D electromagnetic imaging. The wide bandwidth of the receiver also allows time and frequency domain measurements to be made simultaneously. Although not a topic for this discussion, it has been shown that reactions of different liquid organic compounds with clays have varying transient responses to a given stimulus; a measurement tool with a sufficiently wide bandwidth to measure these variations allows the possibility of subsurface contaminant identification.

A wide bandwidth, vector-field sensitive receiver has been developed and field-tested for functionality in geophysical applications. The frequency domain results of the detection of subsurface water flow are discussed herein. The availability of such a receiver allows the possibility of not only detecting a conductivity anomaly such as subsurface water flow but the possible identification of contaminants within the water as well.

Key Words: electromagnetics, giant magnetoresistance (GMR), instrumentation.

INTRODUCTION ●

Geophysical exploration always has an expected target of some sort, even if that target is the background geology. By knowing the expected target characteristics of interest, a geophysical survey may be designed specifically for that target. The survey method used likely represents a degree of compromise between available methods based on suitability to the target, feasibility of method, and cost of method. As a result, there is a limitation to the information any one survey can provide. It is not unusual to find that several surveys of different types are necessary to provide an appropriate answer.

Consider an exploration volume of interest. This volume has an inherent geologic structure having a characteristic set of physical parameters. Geophysical exploration is the process of detecting and measuring those physical parameters and estimating the geologic structure from that information. The presence of fluidic water within the specified exploration volume modifies the inherent geologic background conductivity of the volume. Defining conductivity as a measurement parameter implies that electromagnetic (EM) methods are suitable for exploration and detection.

EM tools are commonly used to detect subsurface contrasts between material conductivities. They are usually simple to construct, easy to use, and provide a relatively quick method for performing geophysical surveys. Subsurface water flow is a particularly easy target in many situations; it is so conductive, it often limits the penetration of geophysical methods looking for different targets.

A traditional EM survey may inject a controlled electric or magnetic field into a desired exploration volume. The source field creates equipotential surfaces within the volume across which a current flows. The amount of current flow is dependent on the conductive properties of the materials within the exploration volume. This current creates secondary magnetic fields around the conductive paths. The magnetic field presents itself at the surface as an upward-oriented field. By measuring the strength of this field and comparing it to the controlled source, some degree of interpretation of the underlying geology within the exploration volume may be obtained. As an illustrative example, consider the following figures:

Figure 1 represents a half cross-section of a heterogeneous exploration volume. The z-axis will be defined as vertical to the earth's surface; the x and y axes will be defined as horizontal to the earth's surface.

The magnetic field presented in this example is symmetrical about the z-axis. A transmitting coil injects a magnetic flux into the earth along the z-axis. This field disperses throughout the exploration volume as indicated. At the earth's surface, the field manifests itself as an upward-directed flux. As the receiver is moved away from the transmitter, the field

Environmental Geosciences, Volume 5, Number 4, 1998 187–195

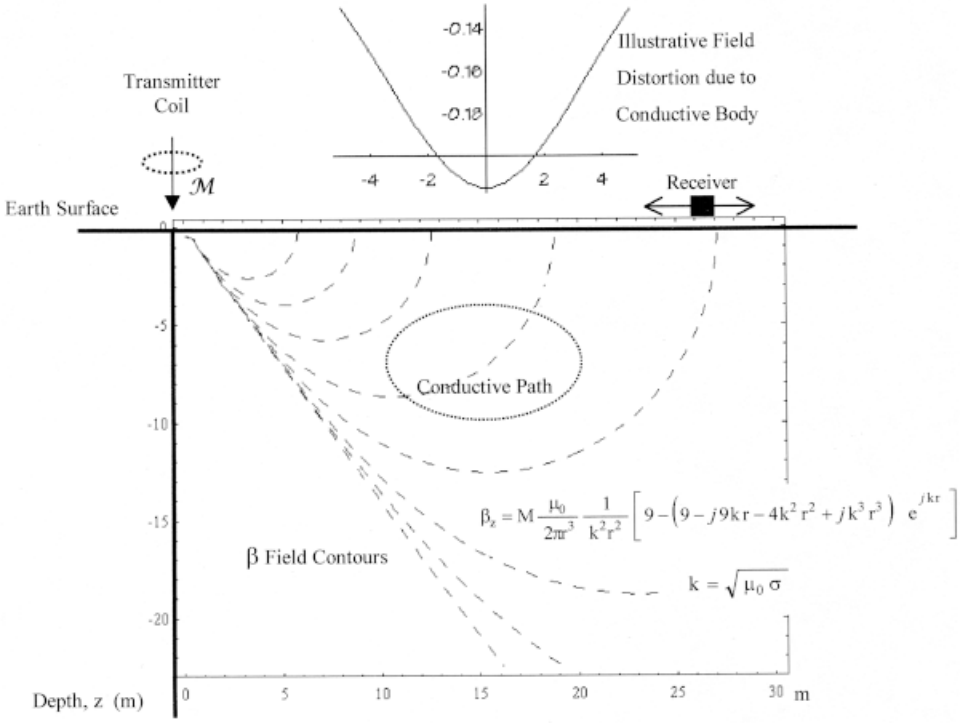

FIGURE 1: Idealized subsurface magnetic field. The presence of a conductive body within the magnetic field would distort the "ideal" field shown here. By using the data collected by the receiver, a deduction of the potential properties of the conductor may be made.

strength decreases, as indicated by the equipotential field strength lines. If there is a more conductive path within the volume as indicated in the figure, the measured field will show a distortion—in this example, a negative anomaly.

Figure 2 illustrates the surface view of the same volume. The same conductive path of the side view of the volume creates a distortion pattern as shown. The stars on the figures represent possible measurement station locations. It is

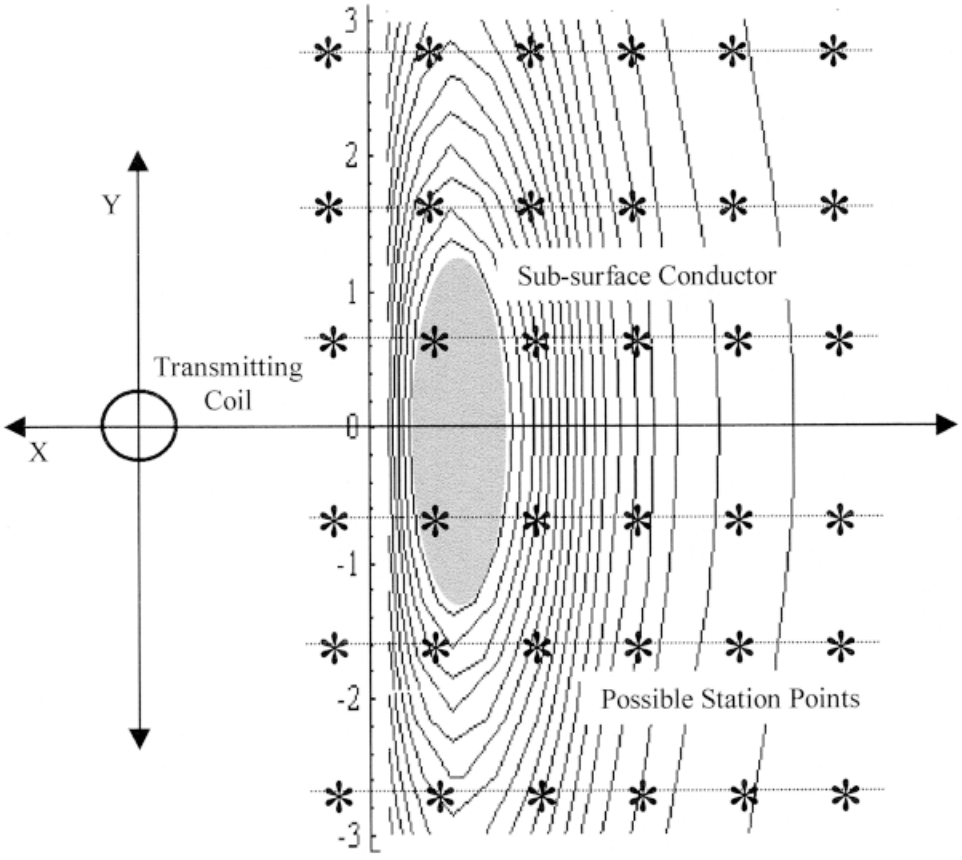

FIGURE 2: Surface view of magnetic field distortion due to subsurface conductive zone. By using device vector capabilities in an array similar to that indicated, the field distortion may be mapped and characteristics of the subsurface conductor may be deduced. By collecting this array data simultaneously, compensation for time-variations in the earth's magnetic field are not necessary.

the goal of the geophysical survey to collect enough data to reproduce the distortion field to a resolution sufficient to define the target. A more complex geology will create a more complex field pattern.

CONDUCTIVITY

Conductivity is the measure of a material's ability to conduct free electrons. Resistivity is the inverse; i.e., the measure of a material's ability to restrict electron movement. Resistivity and conductivity are material properties. It may be assumed that the background geologic structure will have a relatively high resistivity, whereas water will have a low resistivity, particularly if even small amounts of salt are present.

An electron moves in the presence of an electric field; the movement of many electrons is collectively called current. If a current is forced through some volume of interest, it diffuses and flows through the entire volume. The amount of current flowing through any given region of the volume is proportional to the conductivity of the distributed current path.

The magnetic field created by that electron movement is proportional to the amount of current and also diffuses through the material. It should be remembered that current involves a physical movement of matter and that a magnetic field does not. By knowing the parameters of the current source and the strength of the magnetic field at defined intervals of the surface of the exploration volume, some degree of knowledge about the subsurface structure may be deduced.

PHYSICS OF COILS

Coils are commonly used as magnetic field transmitters and receivers. A coil is simple to build, inexpensive to make, and vector-sensitive. Coils are also physically clumsy to maneuver in the field and have a frequency-dependent sensitivity. They do not measure the magnetic field directly; instead, they detect the time-derivative of the field, thereby requiring integration of the data to obtain the magnetic field strength.

As a transmitting device, a coil converts a time-variant current into a time-variant magnetic field, as expressed by the following:

$$\beta_z(t) = \mu n i(t) \frac{a^2}{2(a^2 + z^2)^{3/2}} \qquad (1)$$

where $\beta_z(t)$ is the z-axis component (vertical) of a time-variant magnetic field; μ is the permeability of the medium; n is the number of turns in the coil; i(t) is the time-variant current through the coil; a is the coil radius; and z is the distance along the z-axis between the coil center and the point of interest. For a given coil, variations in the magnetic field are dependent only on the current passing through the coil.

Coils of wire are inductors, mathematically, reactive components with impedance $j\,\omega L$. However, they have significant parasitic resistance and capacitance that defines the frequency characteristics. In mathematical representation, and neglecting parasitic capacitance, a coil impedance can be expressed as $Z_{coil} = R + j\,\omega L$. Of interest here is the quality factor, Q, defined as $\omega_0 L/R$. Q defines the frequency sensitivity of the coil and ω_0 is the resonant frequency of the coil. ω_0 depends on the parasitic capacitance of the coil, is determined by such factors as wire diameter, insulation material and thickness, geometry of the coil construction, and is best determined by empirical methods. Q describes the shape of the frequency response curve; ω_0 defines the resonant frequency.

The parasitic elements of the coil may be estimated using the following approximations. The parasitic resistance is a function of the wire material and size but not the coil geometry, and an accurate determination may be obtained for the value of the resistance analytically. However, the values for the reactive elements, inductance, L, and capacitance, C, are highly dependent on the physical structure of the coil, and the following approximations are mathematical constructs assuming idealistic parameters. Therefore, coil parameters are best determined by empirical methods; the use of measurement equipment appropriate for the frequency range of interest is recommended.

The resistance of the coil is dependent on the conductor. Neglecting temperature effects, the resistance of the coil is found from

$$R = n\rho \frac{1}{A} \qquad (2)$$

where n is the number of turns in the coil; l is the circumference of the coil; A is the cross-sectional area of the conductor, and ρ is the resistivity of the conductor; if copper, ρ = 17.24 nΩ-m. For reference, American Wire Gauge (AWG) No. 10 wire has an approximate resistance of 1 mΩ/ft.

An approximation for the inductance of a coil (Wheeler, 1982) is given by

$$L = \mu n^2 a \left[ln\left(1 + \pi\frac{a}{b}\right) + \frac{1}{2.3 + \frac{1.6b}{a} + 0.44\left(\frac{b}{a}\right)^2} \right] \qquad (3)$$

where a is the coil radius and b is the diameter of the coil cross-section.

If the coil diameter is significantly larger than the wire diameter making up the coil, the parasitic capacitance of the coil may be approximated as

$$C = nl \frac{\pi\varepsilon_r}{ln\frac{2h}{b}} \qquad (4)$$

where n is the number of turns; h is the distance between adjacent centers of the conductors; b is the diameter of the conductor; l is the circumference of the coil, and ε_r is the permittivity of the medium.

The frequency response of a coil with the following parameters is shown in Figure 3. Consider a coil 1 m in diam-

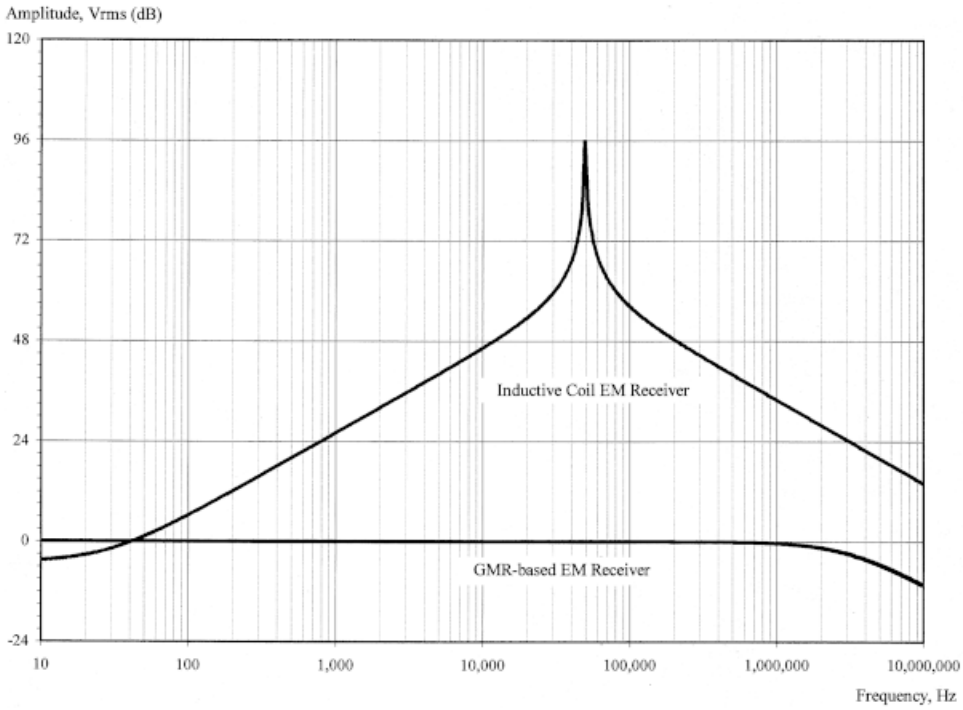

FIGURE 3: Comparative EM receiver frequency response.

eter consisting of 40 turns of AWG No. 10 wire. Assume the wire insulation has a thickness of 25% of the wire diameter. Forty turns will have a cross-section diameter of ~10 cm. The resistance of this coil is ~0.5 Ω, the inductance is found to be ~3.2 mH, and the capacitance is 3.2 nF. This coil's resonant frequency is ~50 kHz. It is obvious that any measurements made with this coil need to be corrected for frequency or that the coil may be used only at a single calibrated frequency.

WIDE-BAND FREQUENCY RESPONSE

When the EM response of a material to a known source is measured over a wide frequency bandwidth, typically several decades, and displayed as amplitude/phase versus frequency, the resulting spectral envelope is referred to as the material's frequency signature. By appropriate analysis and comparison of various frequency signatures, information about the material creating the signature may be derived, which is ultimately the goal of geophysical exploration.

The frequency signature is dependent on certain characteristics of the materials constituting the target as well as the relative concentrations of those materials. Research has indicated significant frequency signature differences between different classes of pollutants and their mixture with water and different clays (Jones, 1997). Ongoing studies also indicate that the potential exists for the individual identification of organic pollutants in a water/clay background (B. Yilmazer, 1998, personal communication).

A frequency signature is also affected by discontinuities of parameters, such as geologic contact zones. To determine advanced target characteristics, measurements over a wide frequency band are desirable. In traditional methods, several coils tuned to different frequencies over the desired bandwidth are necessary. This will require calibration between different coils as well as multiple data sets for each measurement station. A better method would be the use of a wideband receiver that has a constant response over a wide frequency range.

The recent discovery of giant magnetoresistance (GMR) (Baibach, 1988) has led to the development of magnetic field receivers for computer memories and "automatic factories." For these applications, the sensors typically do not have the sensitivities necessary for subtle geophysical measurements. However, an adaptation of this technology has made possible a sensor with both an acceptable signal resolution and frequency response to allow magnetic field measurements over a wide frequency range during a single measurement (McGlone, 1997). A typical frequency response, labeled "GMR-Based Sensor," is also shown in Figure 3. Note that the GMR sensor response assumes no gain in Figure 3 to provide a direct comparison with the response of the illustrative coil. An increase in gain would shift the frequency response curve upward.

FIELD SURVEY

An instrument based on a GMR sensor was given a functionality test under field conditions in the northern Sierra Nevada Mountains. The survey region was an open area of several acres with a known (and normally dry) drainage creek running approximately from west to east. Because of

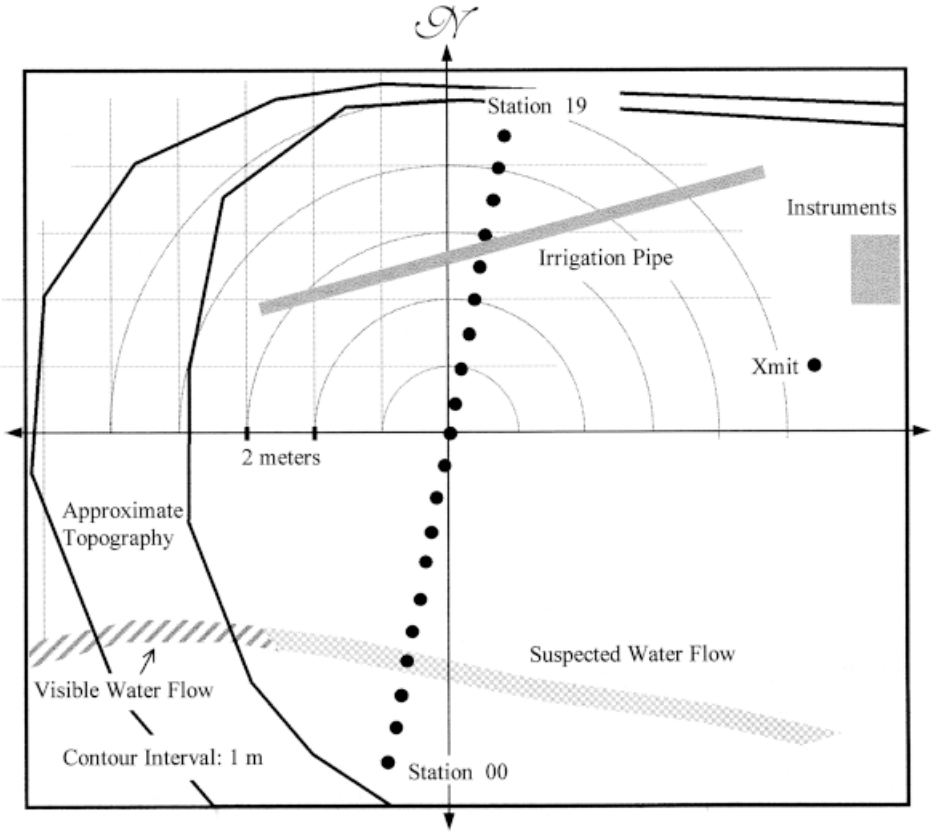

FIGURE 4. Survey plan view (approximately to scale). View of survey area with pertinent features. Target locations based on pre-survey estimates. Contour interval is ∼1 m. Xmit, location of transmitter.

recent rain, there was significant flow in a width of ∼1 m. This creek went underground for some distance; the south end of the survey line crossed the suspected buried path. The goal of this survey was to detect the location of the subsurface flow. It was also thought that a buried, but unused, irrigation pipe was in the area, but this could not be confirmed, and its location was unknown.

The survey area was essentially flat over the entire 19-m survey line but sloped steeply upward at station 19 and sloped upward more gently starting a meter or two south of station 0. Station 0 was designated at the south end of the line; station 19 was at the north end. The survey layout with approximate elevation contours is shown in Figure 4. The geology of this region may be summarized (Mough, 1997) as consisting of Jurassic meta-volcanics with greenschist grade metamorphism. The ground is weakly magnetic, with a fairly uniform distribution of ∼1% magnetite. There is ∼2 m of soil overlaying ∼50 m of well-weathered and fractured rock. The survey line was designed to cross the two suspected anomalies: the small subsurface drainage at or near station 4 with an estimated flow of ∼40 to 60 L/min, and a possible irrigation pipe buried somewhere near the north end.

The source function is a square wave with a fundamental frequency at ∼5 kHz. The transmitter introduced desired, but uncontrolled, distortion and overshoot at the leading edges, providing a pseudo-impulse source function superimposed on the primary square-wave component. The source did not provide a clean signal, and significant harmonic content was readily apparent in the data. The square wave will produce odd harmonics; the triangular nature of the impulses will produce even harmonics.

For this experiment, the data-acquisition equipment was configured to measure signals with frequency content of direct current (DC) to 85 kHz (sample frequency of 170 kHz). A Fast Fourier Transform (FFT) was performed on the data, and the spectral results have a frequency resolution of 167 Hz.

The instrument is sensitive to a single axis with a field resolution of ∼0.3 nT. The instrument was orientated with the sensitive axis oriented in a downward direction (z). The x and y components of the field were not measured during this test sequence; it can be shown analytically that the magnetic field resulting from subsurface conductivity is an upward-directed field at the earth's surface.

The first measurement results are presented in four different views in five figures; Figure 5 presents the data as a 3-D representation of amplitude versus frequency and station number. Figure 6 shows a 2-D "side view" of Figure 5. Figure 7 shows Figure 6 with a logarithmic frequency scale. Figure 8 is a 2-D contour plot of Figure 5. Figure 9 compares the DC response with the response of the primary frequency.

Figure 5 shows very obvious frequency responses that correlate to the locations of the suspected anomalies. The subsurface flow was where expected; the pipe was appar-

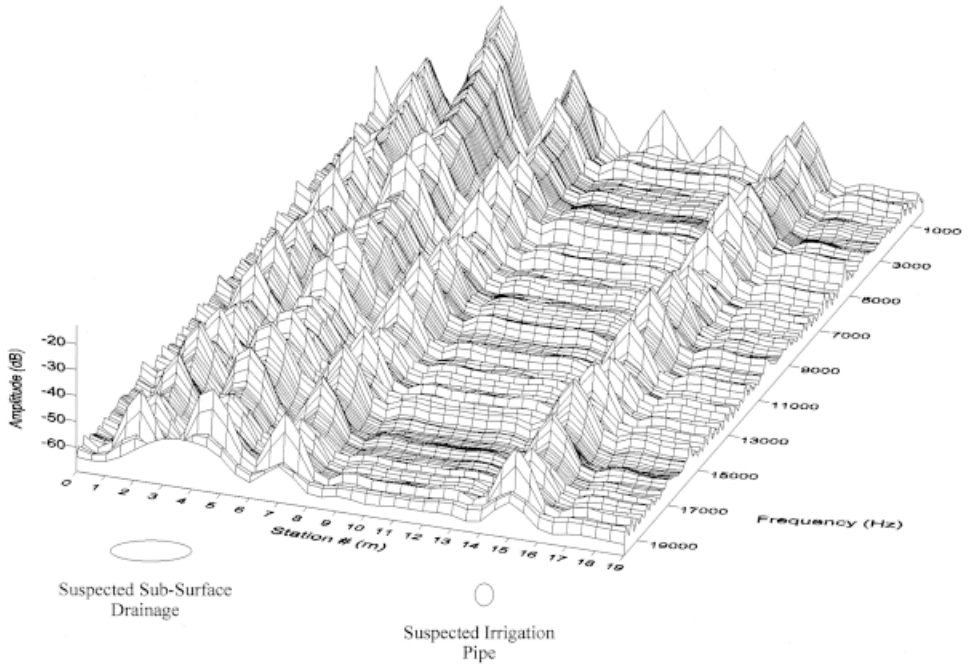

FIGURE 5: Survey results: station spectral amplitude response. Δ Frequency = 167 Hz.

ently near station 15. The measurement "noise floor" is very apparent between stations 8 and 13 as well as between stations 16 and 19.

Figure 6 presents the spectra for each station and the corresponding amplitude. The bottom trace of this figure at –85 dB represents the instrumentation and data-acquisition equipment noise floor in the field. This is not the same as the measurement noise floor of Figure 5. All equipment, including the power generator, was on; the transmitter was connected to power, but the antenna was disconnected. The noise level appears very clean in the frequency band of interest. This indicates little or no signal leakage from the measurement equipment to the sensors.

After connecting the antenna and taking measurements at each station, it was observed that the responses grouped into three sets. The traces at –62 dB are assumed to represent the ambient geophysical noise because the measurement noise floor appears to be at approximately −85 dB. Although

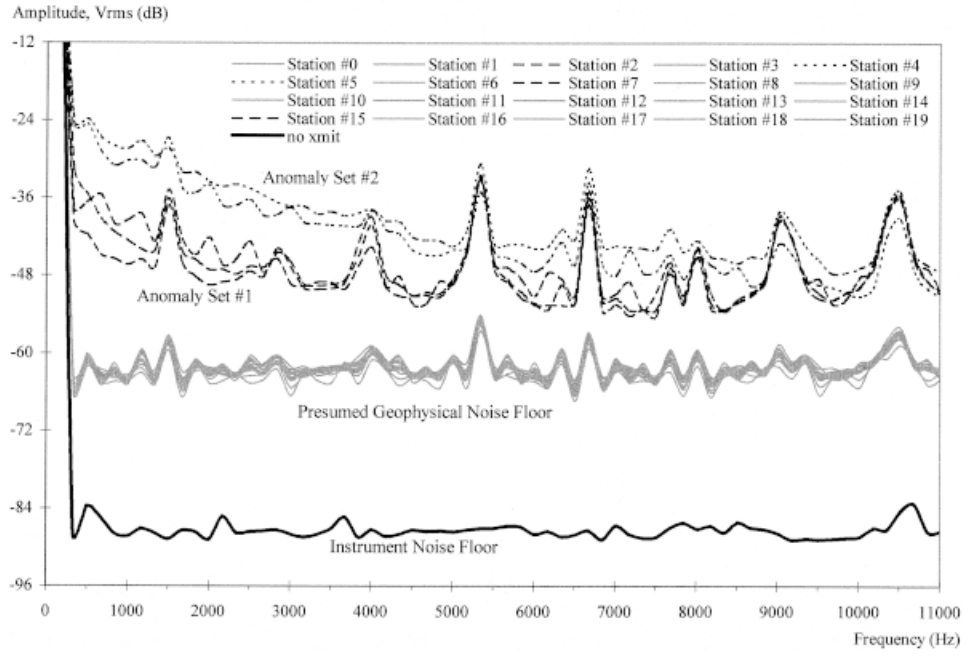

FIGURE 6: Survey results: Station spectral response (linear frequency). Δ Frequency = 167 Hz. Xmit, location of transmitter.

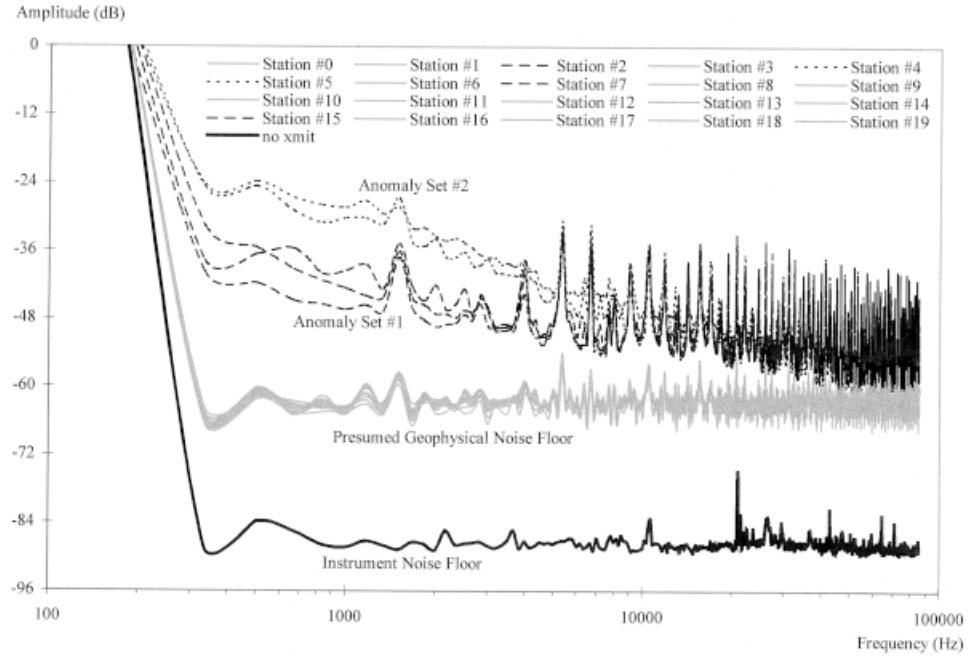

FIGURE 7: Survey results: Station spectral response (log frequency). Δ Frequency = 167 Hz. Xmit, location of transmitter.

there may be a DC magnetic field signature, any frequency-dependent conductivity signature that may be present in this set is contained within the presumed geophysical noise signature and is not detectable at this level of signal processing. It is these stations that make up the surface floor of Figure 5.

The remaining two trace sets show a definite frequency-dependent response. The responses at the fundamental frequency of 5 kHz have almost equal magnitudes and the first harmonic signatures at 10.5 kHz also have large amplitudes, suggesting a material with a high conductivity.

The initial response slopes on the two data sets create frequency signatures that could indicate different depths and/or conductivities. The instrument frequency response capabilities make it feasible to consider these signatures as long late-time responses, as the sample window was ~6 μs. The

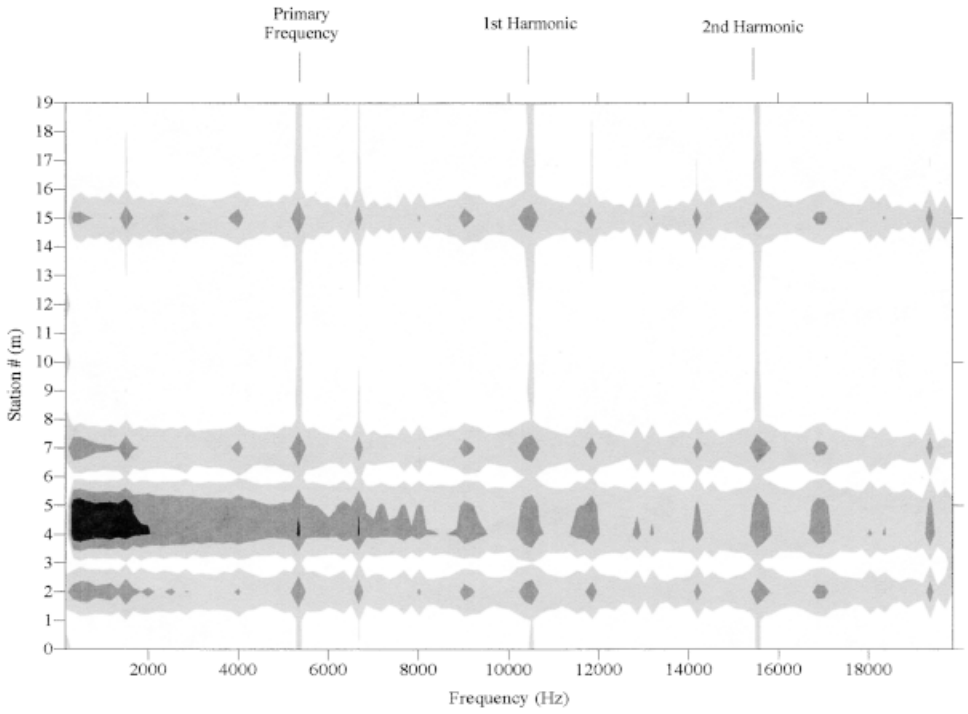

FIGURE 8: Survey results: Amplitude versus frequency surface. DC – 20 kHz.

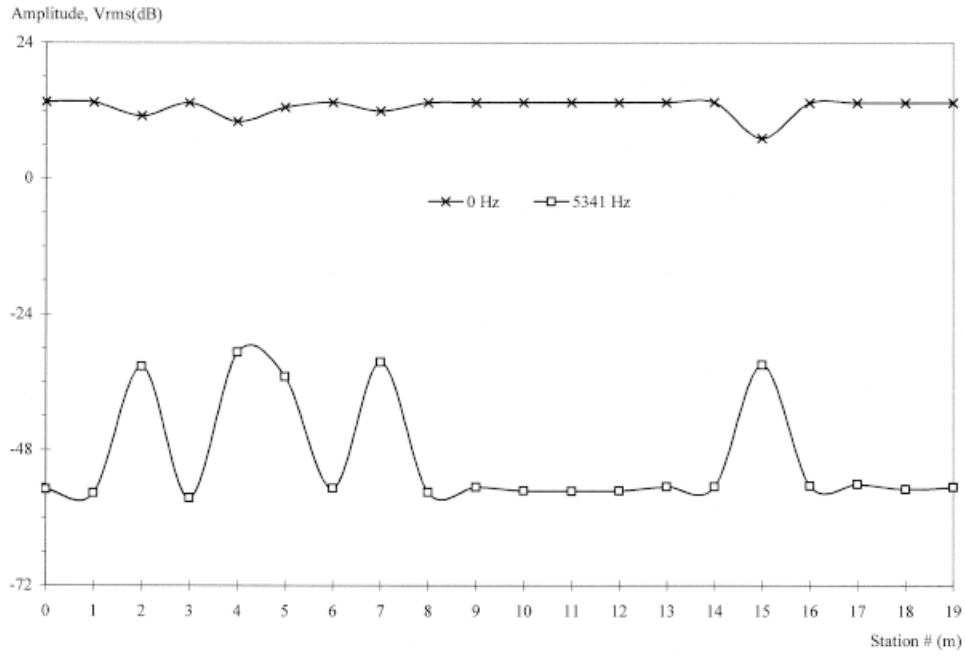

FIGURE 9. Survey results: Magnetic potential field (0 Hz) versus electromagnetic field (5.3 kHz).

noise content introduced by the transmitter has a wide-band frequency spectrum creating sufficient spectral energy to receive a wide frequency-band data set. Because conductors maintain the induced field longer due to less damping, this could be a good indication of high conductivity regions.

Figure 7 is the same as Figure 6 with the exception of being presented with log frequency on the x-axis and extending over the entire frequency range. In this view, the harmonic content is quite apparent, as are the initial frequency roll-off slopes of the two anomalous data sets. The spike in the instrument noise trace at ~21 kHz is an artifact of the data-acquisition equipment. The instrument and presumed geophysical noise floors are essentially flat after an initial decrease in frequency response. However, the traces presumed due to subsurface anomalies seem to show identical slopes at different amplitudes. It appears that these slopes correspond to time-domain responses and that more detailed information in this region could be used to provide further information about the anomalies. A joint time-frequency analysis would be necessary using a data set with finer frequency resolution to investigate these analysis possibilities.

Figure 8 presents the data as a contour of the frequency versus location plane as shown in the surface presentation of Figure 5. Again, the very strong sustained frequencies along the assumed conductive zones stand out quite prominently compared with the quieter locations. This seems to eliminate any significant direct-through-air signal transmission that would tend to have a more uniform amplitude distribution at each station due to the relatively near proximity of the transmitter to all stations. The apparent vertical stripes in Figure 8 are due to the primary source frequencies and are best compared with Figure 5. It is felt that these are insignificant artifacts as they appear in Figure 8, although they provide information about the transmit and receive mechanisms.

Figure 9 compares the DC response with that of the primary transmitter frequency. The data collection process was such that a decrease in the DC curve corresponds to an increased magnetic field strength while an increase in the alternating current (AC) data corresponds to an increased field. The average magnitude in the DC trace is an artifact of the initial nulling process. In this data set, only the relative change in DC response is significant.

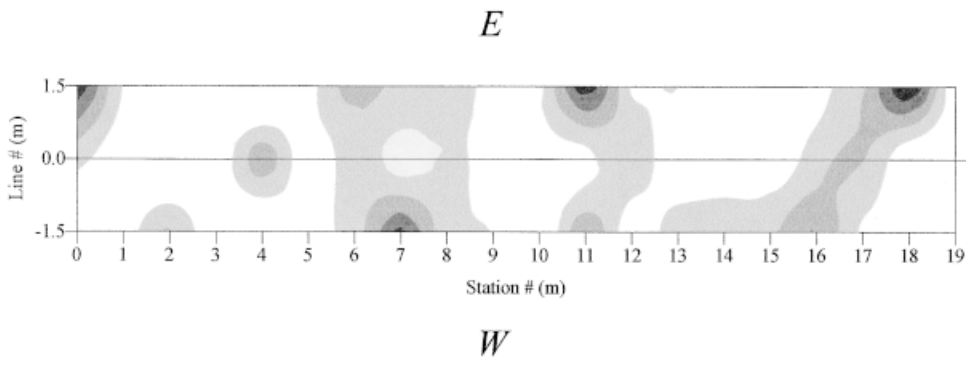

FIGURE 10: Three-line survey results with interpolation.

Whereas there are minor variations in the DC response between stations 2 and 8, the significant anomaly corresponds to the region of the suspected irrigation pipe at station 15. This response would indicate an iron rather than plastic pipe. After the survey, this region was dug up, and a 2.5-cm iron pipe was discovered at a depth of 50 cm. The response at 5 kHz shows strong conduction in the region of stations 2 to 8 where there was minimal ambient magnetization. This appears to confirm the suspected stream path—it appears that the subsurface flow had broken into rivulets. The AC response at station 15 may have a component due to flow in the pipe due to the heavy rains just before the survey, but a steel pipe would appear as a conductive region anyway.

In the interest of examining the potential for a 2-D array, another survey at the same region was completed at a later and drier time. Additional survey lines were measured along lines at 1.5 m on either side of the original line. A contour plot of these results is shown in Figure 10. In retrospect, this data set is insufficient to draw firm conclusions. However, it is possible that this data set shows the irrigation pipe slanting between stations 15 and 18 and that the subsurface flow near station 4 had dissipated.

CONCLUSION ●

The data collected to date seem very encouraging for the possibilities of a magnetic field receiver with a small size and wide frequency response in geophysical exploration. The prototype instrument fits into a package $\sim 15 \times 8 \times 5$ cm^3, making feasible a deployment of EM receiver arrays similar to those currently deployed for seismic exploration. A wide-band EM array could be deployed in a permanent installation, allowing ongoing monitoring of conductive fluid flow within a fixed volume. Use of electronic miniaturization allows the instrument to be deployed in borehole arrays as well.

It now seems feasible to determine variations in conductivity by analysis of frequency signatures. The development of a wide-band instrument that measures magnetic field strength directly as opposed to the detection of the derivative of the field, coupled with current research into electromagnetic signatures of water-clay-pollutant combinations, provides a new method of monitoring and identification of subsurface water flow and possible contaminants.

REFERENCES ●

Baibach, M. N. (1988). Giant magnetoresistance of (001)Fe/(001)Cr magnetic superlattices. *Phys Rev Lett, 61*, 2472–2475.

Jones, D. J. (1997). *Investigation of clay-organic reactions using complex resistivity.* Master's Thesis, Colorado School of Mines, Golden, CO.

McGlone, T. D. (1997). The use of giant magnetoresistance technology in electromagnetic geophysical exploration. In *Proceedings of the Symposium on the Application of Geophysics to Engineering and Environmental Problems* (pp. 705–714). Wheatridge, CO: Environmental and Engineering Geophysical Society.

Mough, D. C. (1997). Mough mineral explorations, Report DCM796. Grass Valley, CA: David C. Mough Mineral Explorations.

Wheeler, H. A. (1982). Inductance formulas for circular and square coils. In *Proceedings of the Institute of Electrical and Electronic Engineers* (pp. 1449–1450). Piscataway, NJ: Institute of Electrical and Electronic Engineers.